TADA: The Topology-Accommodating Direction Assignment Algorithm for Liquid Crystals

Saptarshi Saha,[*,†] Amit Acharya,[*,‡] and Gerald J. Wang[*,†]

†*Department of Civil and Environmental Engineering, Carnegie Mellon University*

‡*Department of Civil and Environmental Engineering and Center for Nonlinear Analysis, Carnegie Mellon University*

E-mail: saptarshisaha@cmu.edu; acharyaamit@cmu.edu; gjwang@cmu.edu

Abstract

Despite the fact that topological defects are a hallmark of liquid crystalline materials, current computational techniques for identifying topological defects in particle-based simulations of these materials – which rest upon Q-tensor theory – do not leverage *topological* features of the system. In this work, we describe the TADA algorithm, a novel approach for identifying disclination cores in liquid crystalline materials, which *is* sensitive to topology: This method assigns to each mesogen a unique vector, thereby extending the concept of the liquid crystal director field down to the scale of mesogens. In systems containing disclination cores, TADA identifies line segments along which this assigned vector field is discontinuous, with cores located at the interior termination points of these line segments. The mere presence of defects can be identified by searching far away from them. We validate this approach by comparing its results to those obtained using the scalar order parameter, for a variety of liquid crystalline assemblies sourced from molecular-dynamics simulations. We also identify several benefits of the TADA algorithm over existing approaches for identifying topological defects in liquid crystalline materials.

Introduction

The primary goal of this work is to develop a computational tool for seamless identification of topological line defects, i.e., disclinations, in liquid crystalline media, without relying on calculations of local ordering. The historical procedure for identifying line defects in nematics may be described as follows (cf. refs.[1,2]): Consider a closed loop in the domain occupied by the nematic. On arbitrarily assigning an orientation to a director at a point on the loop, proceed to assign vector orientations to the director along the loop in a continuous manner. On returning to the "base" point, if the assigned vector orientation of the director is found to be oppositely aligned to how it began, then there must necessarily be a defect of strength 1/2 encircled by the loop. If on the other hand the vector orientation returns to its original direction, then there are either no defects within the loop or an equal number of + and − disclinations encircled by the loop. In this work, we develop a computational implementation of a slight generalization of this simple idea for the identification of disclinations, without relying on the construct of closed loops. Moreover, noting the conceptual absence of any special length-scale in defining the "director" in the above argument, we successfully apply our technique to assemblies of individual mesogens interacting through an inter-mesogen potential.

Our main idea is to assign vector orientations to individual mesogens, as shown in Figure 1. We wish to do so in a manner that is *as continuous as possible* within the domain. Completion of such an assignment over the entire assembly automatically reveals "layers" across which the assigned orientation field has to be discontinuous, provided that there are defects present. Such layers are not uniquely located in space, but nevertheless must be present *somewhere* in the presence of disclinations; they either run from the disclination cores to the boundaries or connect oppositely signed disclinations within the body. While the layers are not uniquely located in space, their terminations must be, and these are the locations of the disclination cores.

The algorithm we develop applies to a director distribution obtained by any means,

experimentally or through simulation or exact solutions of theory of any type.[3,4] A recent class of vector field models for line defects in liquid crystals has been introduced by Zhang *et al.*,[5] making connections with the same class of topological defects in elasticity of solids, and in convection patterns. Our tool is particularly suited for the validation of such models, which explicitly deal with the layer-like features mentioned above. Such models also need, in the definition of their energy density function, a parameter that defines the thickness of these non-unique (in some systems) layers and another that defines the core width of the defects. Our tool explicitly characterizes such length-scales for the higher-scale continuum pde models.

It is worth emphasizing that the approach we develop here is distinct from existing approaches for identifying disclinations in liquid crystalline assemblies. The core difference is that the method described herein is sensitive to topological information, and does *not* depend upon information in the vicinity of each disclination core, whereas existing methods necessarily rely upon kinematic data near the core itself. For example, the core idea employed by Callan-Jones *et al.*,[6] by Slavin *et al.*,[7,8] and by Humpert *et al.*,[9] is to identify disclinations as surfaces along which certain measures of anisotropy (the so-called Westin metrics) take on constant values; however, Westin metrics cannot reveal the presence of a disclination using only data far away from the disclinations. Recent work by Schimming and Viñals[10] takes a different strategy, namely, constructing a quantity (the disclination density) that only takes on non-zero values at disclinations. This approach also successfully identifies disclinations; however, by its nature, it also necessarily requires information in the vicinity of the disclinations themselves. One existing approach with a mild degree of conceptual similarity to our method is described by Zapotocky *et al.*[11] and Billeter *et al.*[12] This approach uses the Q-tensor to guide the creation of a director field, which is evaluated at the corners of a square lattice imposed upon the simulation domain. This approach identifies disclination cores as being present within squares whose corners exhibit a discontinuous flip in director field (a topological insight); however, as with all of the previously described methods, the

signature of a disclination that this method is sensitive to necessarily requires information near the core itself. Moreover, this method requires the selection of a length-scale to set the spacing of the square lattice, and a suitable choice of this quantity depends upon gradients in the order parameter field; the method described below does not involve any choice of such a length-scale.

Methodology

Molecular-Dynamics (MD) Simulations

We validate and test the algorithm developed herein on molecular assemblies obtained from molecular-dynamics (MD) simulations performed in two dimensions using LAMMPS[13] and visualized/post-processed using OVITO.[14] In particular, we study systems containing rod-shaped (calamitic) liquid crystal mesogens, which we treat as ellipsoidal particles interacting via the Gay-Berne (GB) potential,[15,16] a generalization to ellipsoids of the (spherically symmetric) Lennard-Jones potential.[17] Below, we briefly describe this potential; we refer readers interested in full details on the GB potential (as implemented in LAMMPS) to the exposition of Brown.[18] Consider two ellipsoidal particles (indexed as 1 and 2, and assumed to be of equal mass m), whose centers of mass are separated by a distance r. With respect to the laboratory frame, each particle has a relative orientation, which we describe using the (unsigned) vectors $\hat{\mathbf{u}}_\mathbf{1}$ and $\hat{\mathbf{u}}_\mathbf{2}$. For these two particles, their inter-particle potential energy is given by:

$$U(r) = 4\Big(\tilde{\epsilon}(\hat{\mathbf{u}}_\mathbf{1}, \hat{\mathbf{u}}_\mathbf{2}, r)\varepsilon_0\Big)\Big(\tilde{r}^{-12} - \tilde{r}^{-6}\Big) \tag{1}$$

$$\tilde{r} \equiv \frac{r - \tilde{\sigma}(\hat{\mathbf{u}}_\mathbf{1}, \hat{\mathbf{u}}_\mathbf{2}, r) + \sigma_0}{\sigma_0} \tag{2}$$

where ε_0 and σ_0 are (respectively) an energy-scale and a length-scale for the inter-particle interactions, directly analogous to their counterparts for the Lennard-Jones potential. Both

$\tilde{\sigma}(\hat{\mathbf{u}}_\mathbf{1}, \hat{\mathbf{u}}_\mathbf{2}, r)$ and $\tilde{\epsilon}(\hat{\mathbf{u}}_\mathbf{1}, \hat{\mathbf{u}}_\mathbf{2}, r)$ are geometrical terms that account for the relative angle between the two ellipsoids. The quantity $\tilde{r}$ represents the scaled (non-dimensional) distance between the two ellipsoids; it is a function of r (the dimensional distance between the ellipsoid centers of mass), $\tilde{\sigma}(\hat{\mathbf{u}}_\mathbf{1}, \hat{\mathbf{u}}_\mathbf{2}, r)$, and σ_0. In all discussion that follows, we scale all quantities against the length-scale σ_0, energy-scale ε_0, time-scale $\sqrt{m\sigma_0^2/\varepsilon_0}$, density-scale m/σ_0^3, pressure-scale ϵ_0/σ_0^3, and temperature-scale $k_\mathrm{B}/\varepsilon_0$, where k_B is Boltzmann's constant. All mesogens in this work have an aspect ratio (major-axis-to-minor-axis ratio) of 2.5, and all results obtained from computing dynamics employ a timestep of 10^{-3}.

Below, we present results from two broad classes of systems:

1. "Synthetic" geometries: We initialize $1800 \leq N \leq 2000$ mesogens with positions and orientations so as to create a single disclination core in the center of the system. Below, we consider four synthetic geometries ($\pm 1/2$ defects and $\pm$ 1 defects). For the defects of half-integer strength, we work with assemblies that have undergone energy minimization; for the defects of integer strength, we study assemblies that have undergone both energy minimization and dynamics at finite temperature, as described below.

2. "Realistic" geometries: We initialize $N = 8100$ mesogens in a vapor phase (with temperature $T = 50$ and number density $\rho = 0.01$) and then quench the system, making use of the Nosé-Hoover thermostat and barostat,[19,20] to $T = 10^{-3}$ and number density $\rho = 0.45$ (assuming hard ellipsoids with minor axes of length 1 and major axes of length 2.5, this number density corresponds to a packing fraction of approximately 0.87, a couple percent less than the maximum packing fraction possible for ellipsoids[21]). We bound the system along one dimension with two rigid walls made of mesogens, which are (for each wall) all constrained to point in the same direction; for the two walls, these directions are orthogonal to each other, enforcing antagonistic orientational anchoring conditions, as studied in refs.[22,23] The topological defect analysis is carried

out on snapshots obtained after an equilibration period of at least 10 (non-dimensional time units) elapses.

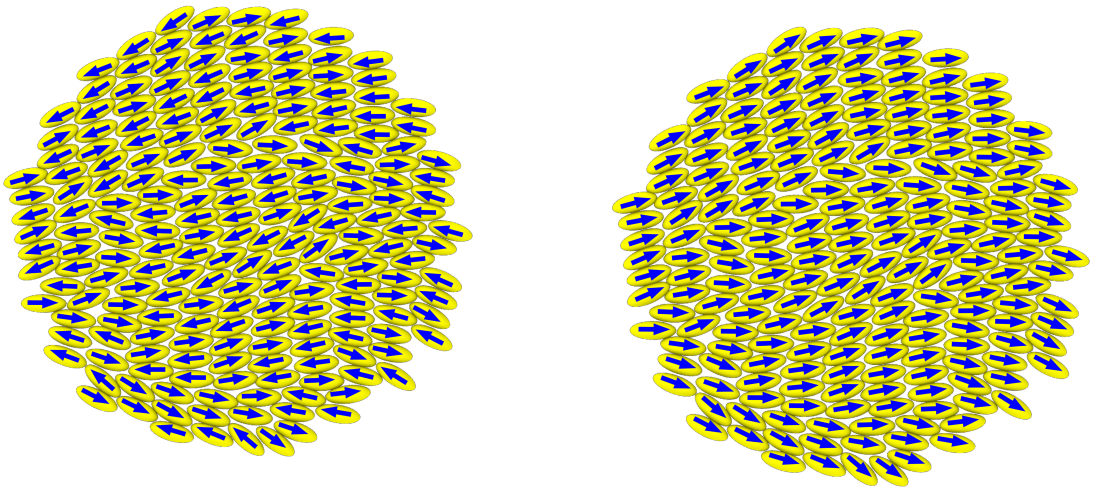

(i) Inconsistent assignment of directions (ii) Consistent assignment of directions

Figure 1: Characteristic equilibrium assembly of a subset ($N = 208$) of mesogens from a "realistic" system. Blue arrows indicate the direction assigned to each mesogen. In (i), these directions are directly obtained from LAMMPS output and are (as expected) topologically inconsistent with each other; in (ii), we show an example of a topologically consistent assignment of directions for this same assembly (all arrows pointing the opposite direction would also qualify as topologically consistent).

TADA Algorithm

Motivated by the importance of *topology*, in this section, we present a novel technique that respects – and helps reveal – the topology of a liquid crystalline assembly. Our approach, termed the Topology-Accommodating Direction Assignment (TADA) Algorithm, assigns each mesogen a direction. We note that any given mesogen possesses a major axis, which corresponds to two possible directions (differing overall by a minus sign). The ultimate goal of this approach is to select one of those two directions to assign to this mesogen (and to carry out this procedure for all mesogens in the system). Before describing the technique itself, it is worth emphasizing several features of this approach:

1. The TADA algorithm approach stands in contradistinction to the much more common assignment of an *unsigned* vector to each mesogen, as is implicitly done for any approach involving Q-tensor theory and the scalar order parameter; for such a representation, there is no distinction between the vectors $\hat{n}$ and $-\hat{n}$.

2. This approach to direction assignment is *not* the same as mapping all vector orientations to a specified semicircular region (i.e., mapping $\hat{n} \rightarrow -\hat{n}$ whenever $\hat{n}$ falls outside of the specified semicircle). Such an approach, by construction, produces directions that are restricted to a subset of the unit circle (and, as a consequence, such an approach is unable to capture topological features, such as the rotation of π in the director field that occurs when traversing a closed loop enclosing a $+1/2$ defect).

We now describe the TADA algorithm:

1. Initialization: Starting from the assembly of liquid crystal mesogens (none of which have been assigned a direction), we select (at random) a single mesogen, and assign it one of the two directions aligned with its major axis (again at random). This assignment of direction (and all subsequent assignments) takes the form of a unit vector.

   We add this mesogen to the List of Assigned Mesogens (LAM) and also to the List of Central Mesogens (LCM).

2. Selection of the next mesogen for consideration and computation of the average local director: For the mesogen most recently added to the LCM, we construct a list of its neighboring mesogens (termed the List of the Most Recent Central Mesogen's Neighbors, or LMRCMN), out to a maximum mesogen center-to-center distance of $d_{\max}$. We sort this list of mesogens from nearest to furthest, relative to the central mesogen. All particles on this list are necessarily either on the LAM or not on the LAM.

   Of the latter (those mesogens not on the LAM), we select the single nearest mesogen to

the mesogen most recently added to the LCM, and designate it as the Mesogen Under Consideration for Assignment (MUCA).

Of the former (those mesogens on the LAM), we compute the average local director $\vec{v}_{\text{ave}}$ as follows:

$$\vec{v}_{\text{ave}} = \frac{1}{M} \sum_{j=1}^{M} \frac{\vec{v}_j}{r_j}, \tag{3}$$

where the index j runs over all M mesogens on the LAM, $\vec{v}_j$ indicates the unit vector assigned to the j-th mesogen, and r_j indicates the center-to-center distance between the MUCA and the j-th mesogen.

3. Vector assignment for the MUCA: Of the two possible direction assignments for the MUCA, we select the direction that makes the smaller angle with $\vec{v}_{\text{ave}}$, and the MUCA is then added to the LAM.

4. Repetition until selection of the next central mesogen: As long as there are still mesogens on the LMRCMN that are not on the LAM, we return to Step 2 (we skip the construction of the LMRCMN, as it has already been constructed).

   Once every mesogen on the LMRCMN has been assigned, we select the first mesogen on the LMRCMN, remove it from the LMRCMN, and add it to the LCM. We then return to Step 2.

   This process continues until all mesogens in the system have been assigned a direction.

5. Identification of disclination cores: After all mesogens have been assigned a direction, a Delaunay triangulation[24] is placed atop the domain, with each mesogen center-of-mass serving as a node. All triangles with any side length exceeding twice the ellipsoid major axis are discarded (such triangles are, without exception, located at the boundaries of the domain). For each triangle, we compute $||\vec{n}_i - \vec{n}_j||$ for each of the three pairs (i, j) of triangle vertices. For any vertex pair where $||\vec{n}_i - \vec{n}_j|| > \delta$, we highlight the two corresponding mesogens. Since the direction assigned to each mesogen takes the form

of a unit vector, the maximum possible value of $||\vec{n}_i - \vec{n}_j||$ is 2, and so δ should be chosen to be slightly less than 2.

Viewed collectively, these highlighted mesogens form a set of continuous line segments. We identify all termination points of these segments that are interior to the domain as disclination cores.

For the results shown below, we use $d_{\max} = 3.5$ and $\delta = 1.8$.

Results and Discussion

We now discuss several results obtained using the TADA algorithm. We start from the synthetic assemblies before moving to the more-realistic cases. Along the way, for the sake of comparison and to highlight contrasts with existing approaches, we also provide calculations of the scalar order parameter making use of the same liquid crystal assemblies.

Synthetic Systems

We first consider four synthetic systems: As a reminder, these systems have been constructed so as to contain solitary disclinations (the four systems are $\pm 1/2$ and ± 1 defects). By construction, in each of the examples shown in this section, the disclination core is located at the center of the image.

We begin with the $\pm 1/2$ cases. Based upon the regions of strong purple coloration located at the center of each image in Figure 2 (where there is a significant difference between individual mesogen orientations and the local average director), we verify that the scalar order parameter can be used to identify defect cores for these simple assemblies.

In Figure 3, we show that TADA can identify the same disclination cores for the $\pm 1/2$ cases. In particular, to verify that TADA is robust to the choice of the initially assigned mesogen, we run the algorithm using four distinct choices for the initially assigned mesogen. In every case, the interior termination point of the highlighted segment is indeed the center

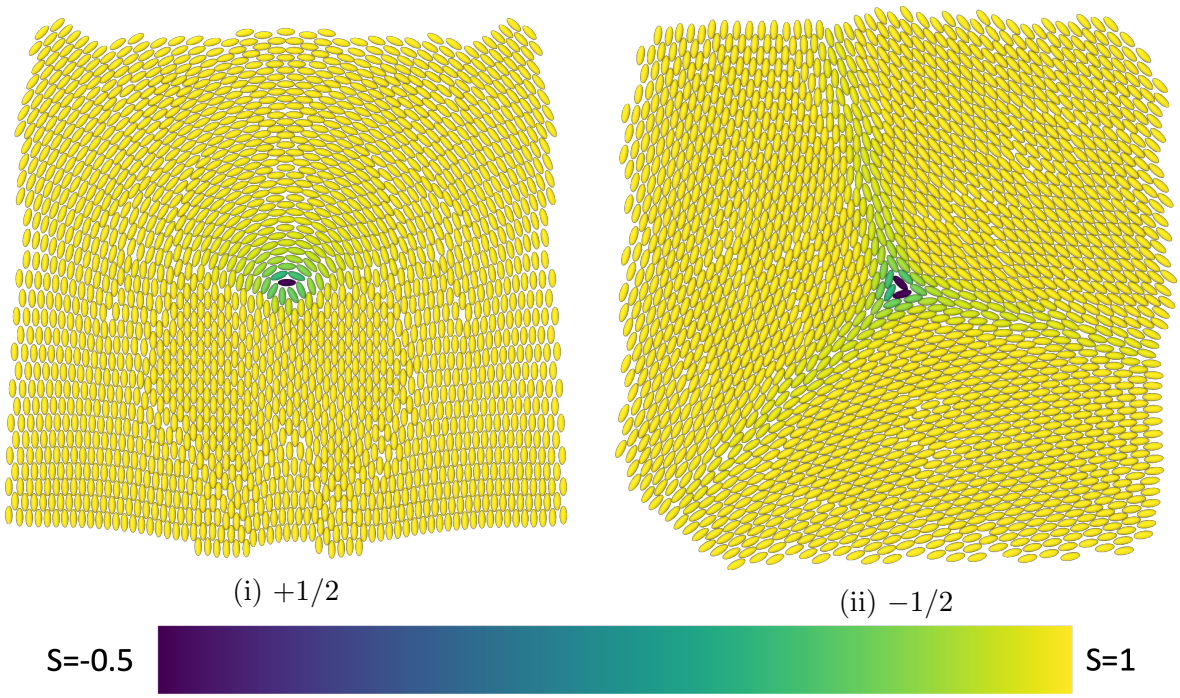

Figure 2: Scalar order parameter for two synthetic assemblies: (i) $+1/2$ defect and (ii) $-1/2$ defect. Defect cores are identifiable as regions of strong purple coloration.

of the domain, at the same location as identified using the scalar order parameter, and also where the defect core was placed by construction. It is worth emphasizing again that the specific location and configuration of the highlighted segment has no physical significance; only its termination point in the interior of the domain carries physical meaning.

We turn now to the case of integer defect strength. Because it is well understood that solitary ± 1 defects are unstable, for these two systems we focus on two snapshots in time: One at a very early time (while the core remains intact) and one after a period of dynamics and subsequent energy minimization (after the core has had sufficient time to split). The results for the scalar order parameter are shown in Figure 4; the results for the TADA algorithm are shown in Figure 5. For both defect types, we observe that at the early stage, both approaches identify the core location to be at the center of the domain (and we can visually verify that the TADA algorithm is robust to the choice of initially assigned mesogen). At the later stage, as expected, both defects with integer topological charge split (for the specific cases visualized, the $+1$ defect splits into two $+1/2$ defects that migrate along a

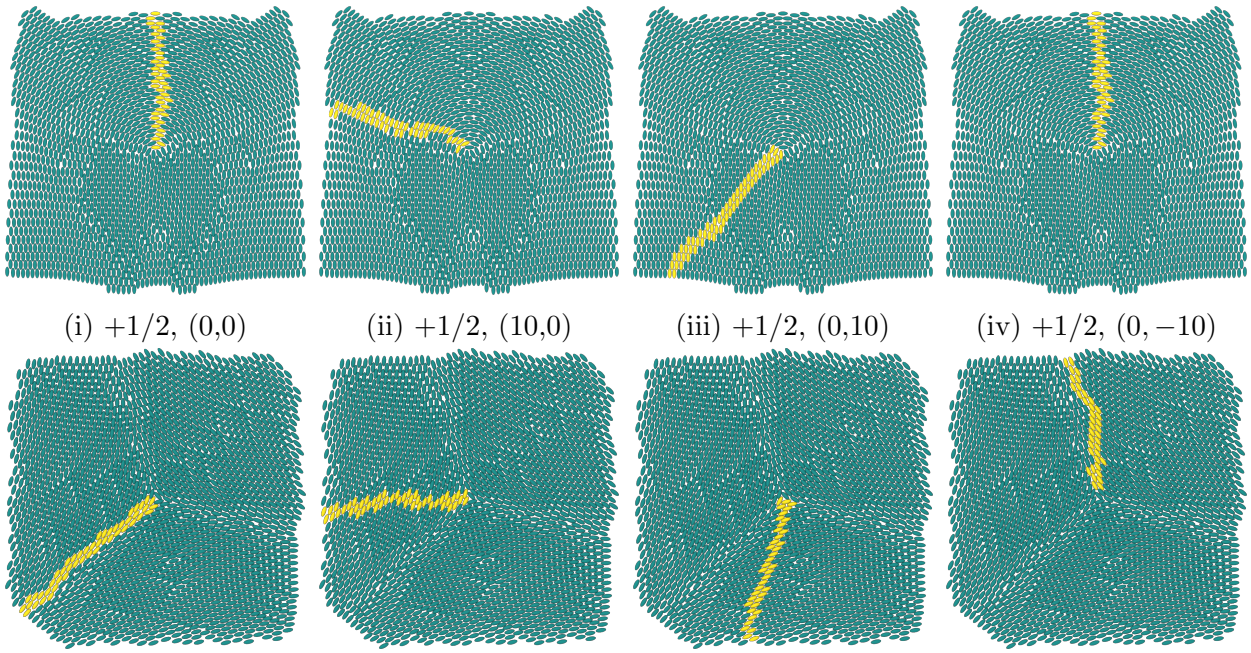

Figure 3: Application of the TADA algorithm to identify defect cores for (i-iv) $+1/2$ defects and (v-viii) $-1/2$ defects; disclination cores are located at the interior point of termination of each yellow segment. In each column of figures, we specify the spatial coordinates for the initially assigned mesogen, which is different for each column.

roughly north-south axis and the -1 defect splits into two $-1/2$ defects that migrate along a roughly east-west axis). Both methods successfully identify this splitting; in particular, the TADA algorithm generates a series of highlighted segments, which produce a set of interior termination points close to the defect core regions identified using the scalar order parameter.

We observe that at the later stage, there is a small amount of discernible variability in the defect core locations identified using the TADA algorithm, which depends upon the choice of initial mesogen. This phenomenon is clearest in Figure 5 for the -1 defect. Nevertheless, for all choices of initially assigned mesogen, the maximum discrepancies in observed core location are comparable to the length of a single mesogen, which (it is worth noting) is comparable to the uncertainty in core location using the scalar order parameter (since the region where S takes on its most negative values is not localized to a single mesogen).

(More) Realistic Systems

We turn now to an assembly of higher complexity, which (as a reminder) was obtained by rapidly quenching and compressing a mesogen vapor into a condensed phase. We expect *a priori* that such a system will feature a wealth of disclinations, not generally amenable to identification by visual inspection. In Figure 6, we show that both techniques generally identify the same defect cores, with discrepancies that are at most on the order of a single mesogen length.

Relative Merits of the TADA Algorithm

Having verified that the TADA algorithm can identify the same disclinations as the scalar order parameter (modulo at most one mesogen length), we now discuss the advantages of the TADA algorithm *vis-à-vis* the scalar order parameter. It is worth emphasizing at the outset of this discussion that the TADA algorithm directly follows in the footsteps of the historical (and topologically focused) approach, as discussed in the Introduction. However, beyond merely being grounded in the historical approach, we identify two key capabilities

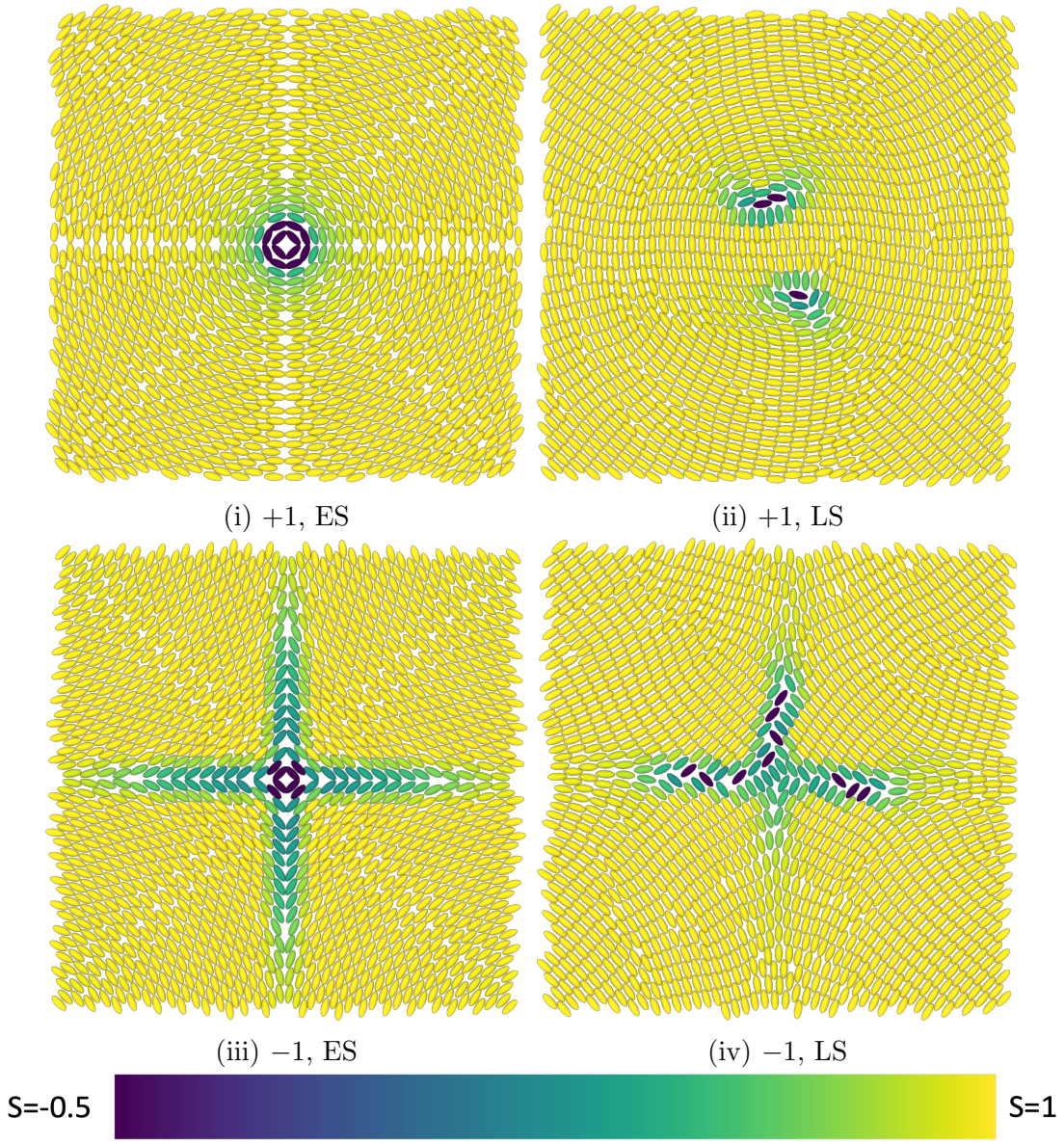

Figure 4: Application of the scalar order parameter to identify disclination cores for (i-ii) +1 defects and (iii-iv) −1 defects. The first column shows early-stage (ES) configurations, prior to core splitting; the second column shows later-stage (LS) configurations, after core splitting.

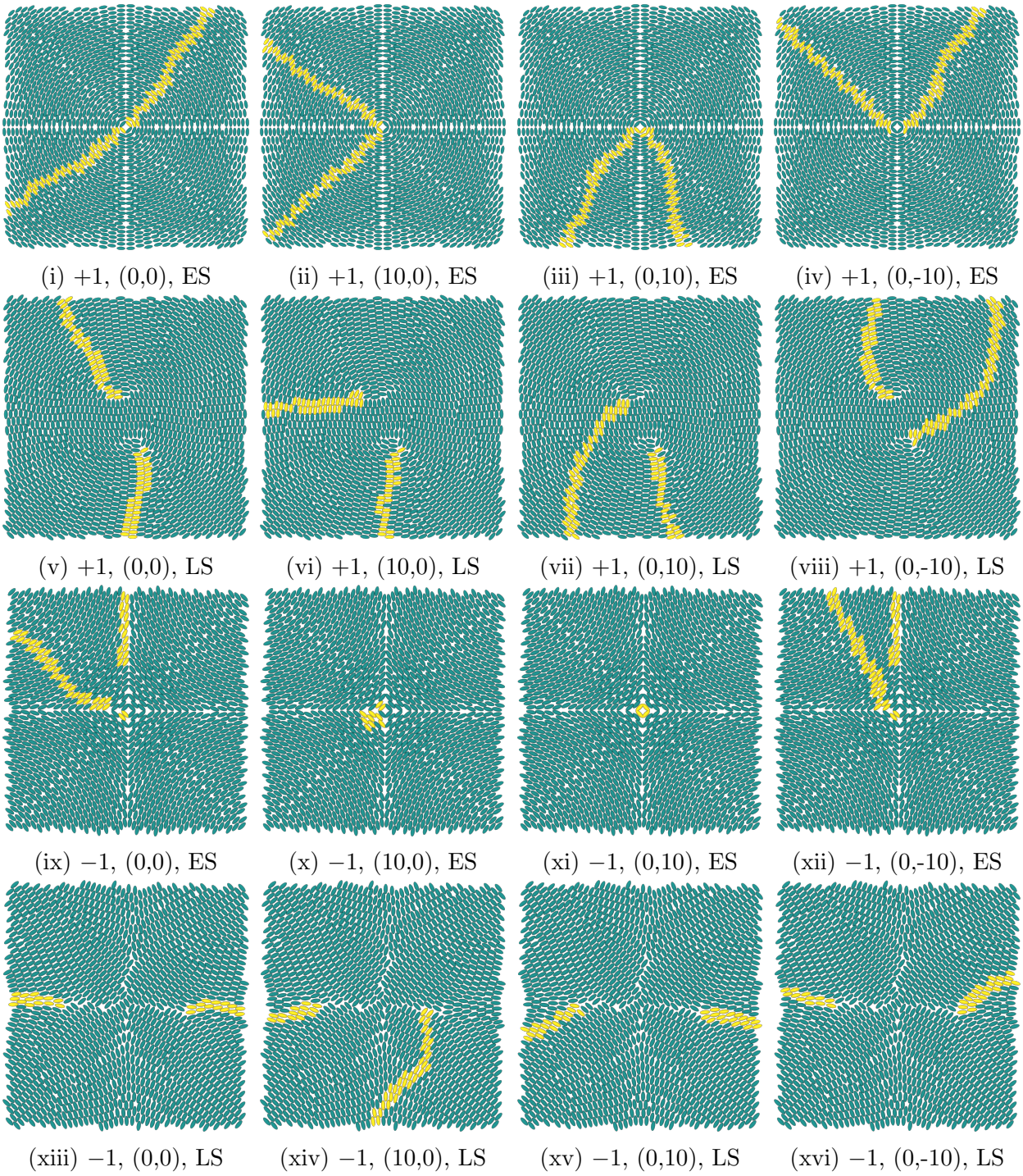

Figure 5: Application of the TADA algorithm to identify cores for (i-viii) +1 defects and (ix-xvi) −1 defects; cores are located at the interior points of termination of yellow segments. The first and third rows show early-stage (ES) configurations, prior to core splitting; the second and fourth rows show later-stage (LS) configurations, after core splitting. In each column of figures, we choose a different coordinate for the initially assigned mesogen.

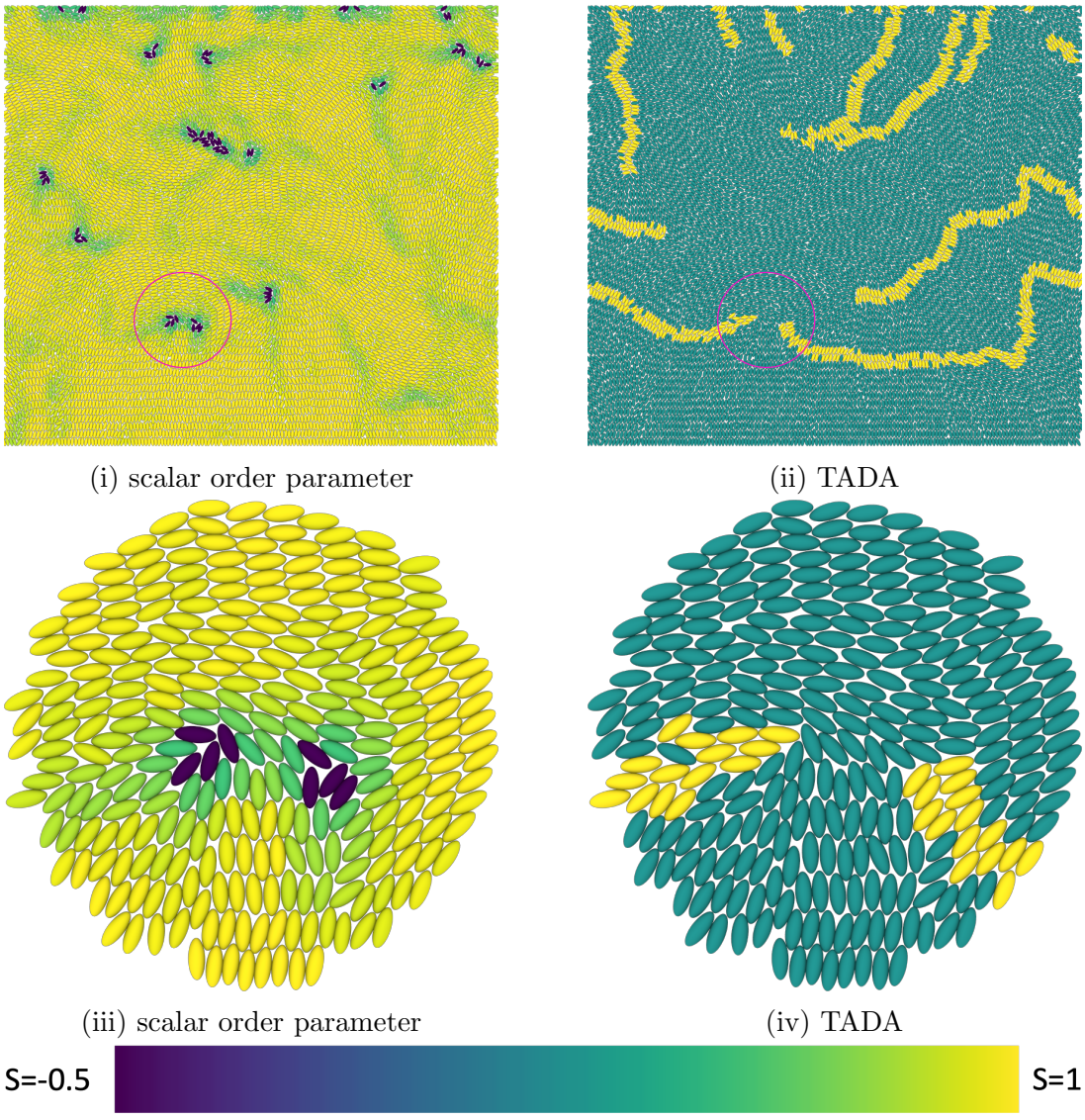

Figure 6: For a realistic configuration of mesogens, identical disclinations identified via (i) the scalar order parameter and (ii) the TADA algorithm. In (iii) and (iv), we provide close-up views of the region circled in pink in (i) and (ii), containing two disclination cores. The color bar shows the range for the scalar order parameter.

only possessed by the TADA algorithm.

Intermediate-Stage Identification of Defect Core Splitting

As shown in Figures 4 and 5, both the TADA algorithm and the scalar order parameter are capable of revealing eventual core splitting for integer-charge topological defects. Here, we call attention to a (potentially unsurprising, but nevertheless noteworthy) strength of TADA: At intermediate times, just as the disclination core is beginning to split, TADA unambiguously identifies the split before it is clear using the scalar order parameter, which instead highlights a large region of disorder (Figure 7). This result suggests that the TADA algorithm is better suited for tracking defect evolution with fine spatiotemporal resolution.

Defect Identification in Cases of Limited Information

Yet another advantage of the TADA algorithm is that it can infer the presence of a disclination core in a region *even when no data is provided in the vicinity of the core itself.* In Figure 8, we show the TADA algorithm and the scalar order parameter for synthetic assemblies corresponding to the four topological charges previously studied; in each case, a certain portion of the dataset containing the core itself has been excised from the dataset. Whereas the scalar order parameter is blind in all cases to the presence of a disclination (it is sensitive only to *local* disorder in the vicinity of a defect), in every case with a $\pm 1/2$ strength defect, the TADA algorithm produces a highlighted segment that terminates in the interior of the domain, on the boundary of the excised region (indicating the presence of a core *somewhere* within this region). In other words, the TADA algorithm is truly sensitive to topological considerations, and does not require information near the core itself to deduce that the region in which data is missing contains a net topological charge with non-integer magnitude. (In cases where the region in which data is missing has a non-zero and integer topological charge, it is possible to either see multiple lines terminating on the boundary of the excised region or none.) It is worth noting that this analysis compares favorably to –

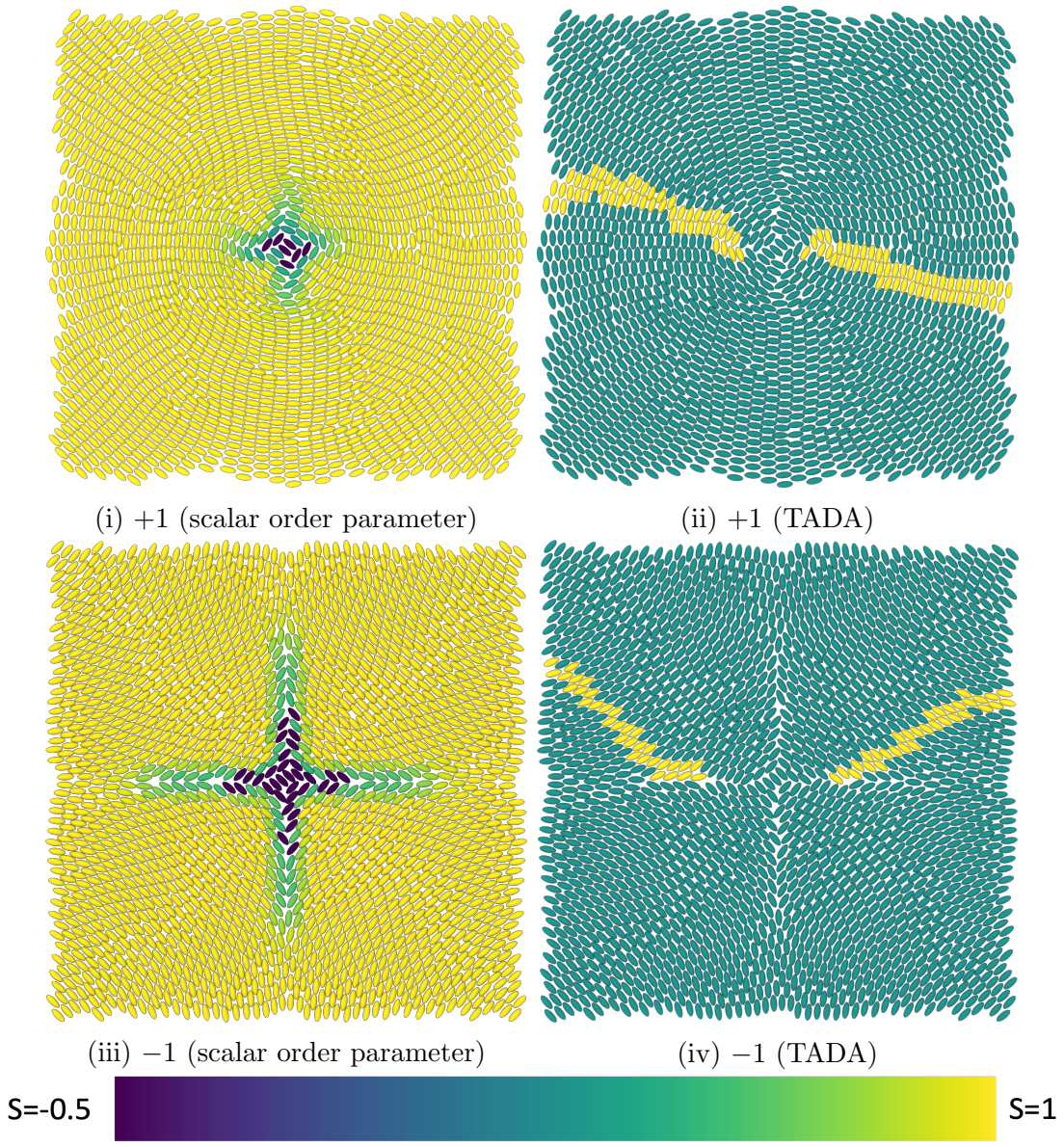

Figure 7: Disclination core splitting at an intermediate stage (shortly after the core begins to split), for (i) +1 (scalar order parameter); (ii) +1 (TADA); (iii) −1 (scalar order parameter); and (iv) −1 (TADA). The color bar shows the range for the scalar order parameter.

and is in fact directly inspired by – the arguments in Section IIB of the landmark article by Mermin.[2]

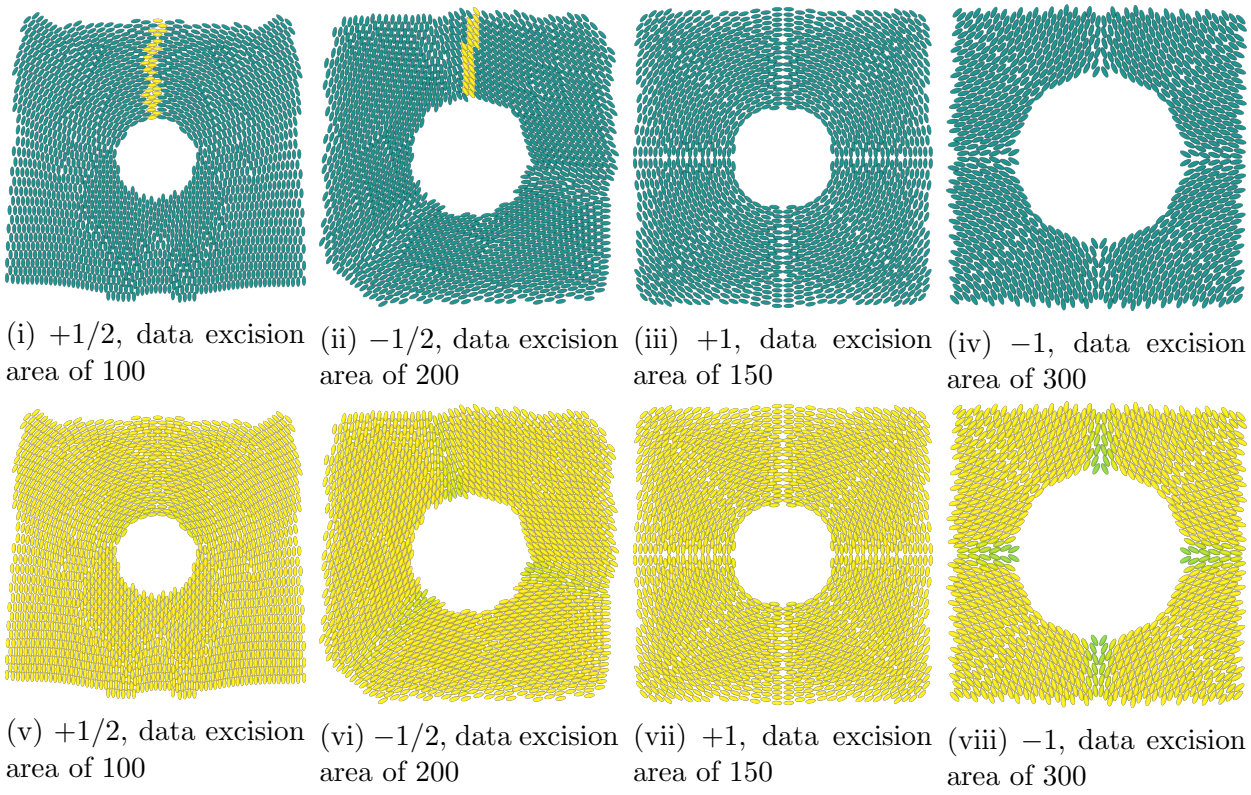

(i) $+1/2$, data excision area of 100 (ii) $-1/2$, data excision area of 200 (iii) $+1$, data excision area of 150 (iv) -1, data excision area of 300

(v) $+1/2$, data excision area of 100 (vi) $-1/2$, data excision area of 200 (vii) $+1$, data excision area of 150 (viii) -1, data excision area of 300

Figure 8: Identification of defects within four synthetic assemblies, each with a specified amount of data removed from the overall dataset. The top row (i-iv) shows results from the TADA algorithm; the bottom row (v-viii) shows results from the scalar order parameter.

We close our discussion by noting yet another advantage of TADA, based upon its suitability for use with efficient statistical sampling techniques. In principle, one could start from a trivially topologically consistent configuration (e.g., a smectic assembly of mesogens with all directions assigned to the north) and then obtain defected assemblies only through "gentle" perturbations/deformations of this initial configuration (here, "gentle" means that no mesogen ever experiences a force or torque sufficiently large to cause it to flip to an inconsistent direction within an otherwise ordered domain). Although such an approach would ultimately produce a vector field of directions identical to those generated by TADA, TADA opens the door to the use of non-physical decorrelation methods (via, e.g., high-temperature dynamics[25]); this is because TADA "works from a clean slate" each time it assigns directions,

and is thus completely unaffected if it is initially fed a grossly inconsistent set of directions. Such enhanced-sampling methods are critical for generating statistically representative ensembles of configurations, especially for materials with large correlation length-scales and long correlation time-scales, as is frequently the case for liquid crystals.

Conclusion

We have developed a novel approach – the Topology-Accommodating Direction Assignment (TADA) algorithm – for assigning a vector field of directions to any assembly of liquid crystal mesogens in a manner that is *as continuous as possible for that assembly.* In assemblies where this is not possible, the discontinuities identified by this algorithm form line segments, whose termination points interior to the domain represent topological defects. This strategy demonstrates that it is possible (and in fact highly fruitful) to extend the concept of a director field down to the length-scale of individual mesogens within liquid crystalline media, without making any reference to a local order parameter quantity.

We have validated the TADA algorithm by comparison to disclination cores identified using the scalar order parameter, for a large variety of assemblies. In all cases, we find agreement up to the length of a single mesogen. We have also discussed several distinctive strengths that the TADA algorithm exhibits: Chief among these are the ability to unambiguously identify core splitting earlier than the scalar order parameter and the ability to infer the presence of a disclination in the presence of limited data near the core itself.

There are several natural avenues to develop and leverage the TADA algorithm, which will be the subject of future work. At a basic level, all of the results and analysis herein focused on the two-dimensional case; it would be natural to extend TADA to three dimensions, enabling the identification of disclination *lines* running through the body of a liquid crystalline assembly. The TADA algorithm also generates precisely the geometrical and topological information needed to calibrate and test a recent class of continuum models

proposed for line defects in liquid crystals.[5] As such, the TADA algorithm is also a promising technique for supplying nanoscale detail to macroscale models, enabling accurate and efficient multi-scale modeling of liquid crystalline materials.

Acknowledgement

The authors gratefully acknowledge conversations with Alexander Stukowski regarding the efficient use of the software OVITO. The authors also gratefully acknowledge computing resources funded by the Carnegie Mellon University (CMU) College of Engineering and the CMU Department of Civil and Environmental Engineering. This work was supported by the National Science Foundation under Grant 2021019.

References

(1) Kleman, M.; Lavrentovich, O. D. *Soft Matter Physics: An Introduction*; Springer New York: New York, NY, 2003.

(2) Mermin, N. D. The topological theory of defects in ordered media. *Rev. Mod. Phys.* **1979**, *51*, 591–648.

(3) De Gennes, P.-G.; Prost, J. *The physics of liquid crystals*; Oxford university press, 1993.

(4) Sigillo, I.; Greco, F.; Marrucci, G. Model of a disclination core in nematics. *Liquid Crystals* **1998**, *24*, 419–425.

(5) Zhang, C.; Acharya, A.; Newell, A. C.; Venkataramani, S. C. Computing with non-orientable defects: Nematics, smectics and natural patterns. *Physica D: Nonlinear Phenomena* **2021**, *417*, 132828.

(6) Callan-Jones, A.; Pelcovits, R. A.; Slavin, V.; Zhang, S.; Laidlaw, D.; Loriot, G. Simulation and visualization of topological defects in nematic liquid crystals. *Physical Review E* **2006**, *74*, 061701.

(7) Slavin, V.; Pelcovits, R.; Loriot, G.; Callan-Jones, A.; Laidlaw, D. Techniques for the visualization of topological defect behavior in nematic liquid crystals. *IEEE transactions on visualization and computer graphics* **2006**, *12*, 1323–1328.

(8) Slavin, V. A.; Laidlaw, D. H.; Pelcovits, R.; Zhang, S.; Loriot, G.; Callan-Jones, A. Visualization of topological defects in nematic liquid crystals using streamtubes, streamsurfaces and ellipsoids. IEEE Visualization 2004. 2004; pp 21p–21p.

(9) Humpert, A.; Brown, S. F.; Allen, M. P. Molecular simulations of entangled defect structures around nanoparticles in nematic liquid crystals. *Liquid Crystals* **2018**, *45*, 59–69.

(10) Schimming, C. D.; Viñals, J. Singularity identification for the characterization of topology, geometry, and motion of nematic disclination lines. *Soft Matter* **2022**, *18*, 2234–2244.

(11) Zapotocky, M.; Goldbart, P. M.; Goldenfeld, N. Kinetics of phase ordering in uniaxial and biaxial nematic films. *Phys. Rev. E* **1995**, *51*, 1216–1235.

(12) Billeter, J. L.; Smondyrev, A. M.; Loriot, G. B.; Pelcovits, R. A. Phase-ordering dynamics of the Gay-Berne nematic liquid crystal. *Phys. Rev. E* **1999**, *60*, 6831–6840.

(13) Thompson, A. P.; Aktulga, H. M.; Berger, R.; Bolintineanu, D. S.; Brown, W. M.; Crozier, P. S.; in 't Veld, P. J.; Kohlmeyer, A.; Moore, S. G.; Nguyen, T. D.; Shan, R.; Stevens, M. J.; Tranchida, J.; Trott, C.; Plimpton, S. J. LAMMPS - a flexible simulation tool for particle-based materials modeling at the atomic, meso, and continuum scales. *Comp. Phys. Comm.* **2022**, *271*, 108171.

(14) Stukowski, A. Visualization and analysis of atomistic simulation data with OVITO – the Open Visualization Tool. *Modelling and Simulation in Materials Science and Engineering* **2010**, *18*.

(15) Gay, J. G.; Berne, B. J. Modification of the overlap potential to mimic a linear site-site potential. *The Journal of Chemical Physics* **1981**, *74*, 3316–3319.

(16) Berardi, R.; Fava, C.; Zannoni, C. A Gay-Berne potential for dissimilar biaxial particles. *Chemical Physics Letters* **1998**, *297*, 8 – 14.

(17) Allen, M. P.; Tildesley, D. J. *Computer Simulation of Liquids*; Oxford University Press, 1989.

(18) Brown, M. Additional documentation for the Gay-Berne ellipsoidal potential as implemented in LAMMPS. 2007.

(19) Nosé, S. A unified formulation of the constant temperature molecular dynamics methods. *The Journal of chemical physics* **1984**, *81*, 511–519.

(20) Hoover, W. G. Canonical dynamics: Equilibrium phase-space distributions. *Physical review A* **1985**, *31*, 1695.

(21) Delaney, G.; Weaire, D.; Hutzler, S.; Murphy, S. Random packing of elliptical disks. *Philosophical Magazine Letters* **2005**, *85*, 89–96.

(22) Janning, J. L. Thin film surface orientation for liquid crystals. *Applied Physics Letters* **1972**, *21*, 173–174.

(23) Ramezani-Dakhel, H.; Sadati, M.; Rahimi, M.; Ramirez-Hernandez, A.; Roux, B.; de Pablo, J. J. Understanding Atomic-Scale Behavior of Liquid Crystals at Aqueous Interfaces. *Journal of Chemical Theory and Computation* **2016**, *13*, 237–244.

(24) Virtanen, P. et al. SciPy 1.0: Fundamental Algorithms for Scientific Computing in Python. *Nature Methods* **2020**, *17*, 261–272.

(25) Li, Y.; Wang, G. J. How to produce confidence intervals instead of confidence tricks: Representative sampling for molecular simulations of fluid self-diffusion under nanoscale confinement. *The Journal of Chemical Physics* **2022**, *156*, 114113.